

Interacting valence holes in *p*-type SiGe quantum disks in a magnetic field

Luis G. C. Rego,* Pawel Hawrylak, Jose A. Brum,* and Arkadiusz Wojs,†

Institute for Microstructural Sciences, National Research Council of Canada, Ottawa, Canada K1A 0R6

(Received 4 June 1996)

The interaction of holes in *p*-type SiGe quantum disks in a magnetic field is studied. The holes are described by a Luttinger Hamiltonian, with parity replacing spin as a good quantum number. The interaction Hamiltonian separates into charge-charge and parity-parity parts. The effect of parity mediated hole-hole interactions is illustrated by numerical calculations of the energy and capacitance spectra for up to two holes in a quantum disk for parameters corresponding to a SiGe system. [S0163-1829(97)04523-2]

I. INTRODUCTION

There is currently interest in SiGe based quantum confined semiconductor nanostructures, such as quantum disks,¹ self-organized dots,² and submicrometer tunneling diodes^{3,4} compatible with existing silicon technology.⁵ The SiGe systems differ from the heavily studied GaAs system in a number of ways. Unlike in GaAs, in SiGe based quantum wells electrons are, at best, weakly confined⁶ and only valence band holes show significant quantum confinement effects. Since current technology allows for charging nanostructures with individual electrons⁷⁻⁹ one might expect to study in the near future strongly interacting holes in SiGe nanostructures. We therefore investigate here the effect of hole-hole interaction in SiGe quantum disks built from a symmetric quantum well (QW), including the effect of the magnetic field.

Some aspects of quantum confinement on valence band holes have already been investigated. The single particle spectrum of holes in GaAs quantum boxes¹⁰ and quantum dots with parabolic confinement, including magnetic field, have been investigated.¹¹ The effect of finite hole density and hole-hole interaction on absorption of infrared radiation has been investigated within the local density approximation.¹² The effect of confinement on the two-hole spectrum has also been investigated.¹³ Much of the theoretical work on holes in quantum dots paralleled theoretical and experimental work on electrons.¹⁴ For example, it has been shown recently that interesting physics in double-layer quantum dots can be traced back to electron ‘‘isospin.’’¹⁵ We will show that when valence holes are described by a Luttinger Hamiltonian, interesting physics arises in single-layer valence hole systems associated with parity replacing spin as a good quantum number. The interaction Hamiltonian then separates into a charge-charge and parity-parity parts, in analogy with double-layer systems.^{15,16} We illustrate the effect of parity mediated hole-hole interactions by numerical calculations of the energy and capacitance spectrum of two holes in a quantum disk for parameters corresponding to a SiGe system.

II. SINGLE HOLE IN A QUANTUM DISK

The spin-orbit interaction couples the hole orbital angular momentum and its spin. The hole states are described in terms of their total angular momentum \vec{J} , where $J = \frac{3}{2}, \frac{1}{2}$. The set of solutions with $J = \frac{3}{2}$ and z projections $J_z = \pm \frac{3}{2}, \pm \frac{1}{2}$

correspond to the heavy-hole bands (HH) and light-hole bands (LH), respectively. The states with $J = \frac{1}{2}$ and $J_z = \pm \frac{1}{2}$ correspond to the split off bands (SO). At finite values of the wave vector \mathbf{k} , these bands are coupled. The SO bands are not included in our model because they are separated in energy from HH and LH bands and have only a small influence on the behavior of the heavy- and light-hole bands.¹⁷ For infinite barriers, the effect of strain reduces to a rigid shift of the heavy- and light-hole subbands and cannot be distinguished from the effect of the finite thickness of the disk. We therefore introduce an effective thickness w of the QW which could be chosen to give the actual heavy- and light-hole ground states separation in a strained sample.

Because we are interested in many-body effects we assume a simple model of confinement yielding simple wave functions. We assume that holes are confined in a cylindrical disk of radius r and thickness w surrounded by infinite potential barriers. An external magnetic field B is applied along the z direction, perpendicular to the plane of the disk. The Zeeman effect is neglected in our calculations.

The light- and heavy-hole states are described by a Luttinger-Kohn Hamiltonian:^{18,19}

$$H_L = \begin{pmatrix} P_+ & R & -S & 0 \\ R^* & P_- & 0 & S \\ -S^* & 0 & P_- & R \\ 0 & S^* & R^* & P_+ \end{pmatrix}, \quad (1)$$

where H_L is spanned in the basis $J = \frac{3}{2}, J_z = \frac{3}{2}, -\frac{1}{2}, \frac{1}{2}, -\frac{3}{2}$. The matrix elements of the Luttinger Hamiltonian (1) are

$$P_+ = \frac{\hbar^2}{2m_0} [(\gamma_1 - 2\gamma_2)k_z^2 + (\gamma_1 + \gamma_2)k_\rho^2], \quad (2)$$

$$P_- = \frac{\hbar^2}{2m_0} [(\gamma_1 + 2\gamma_2)k_z^2 + (\gamma_1 - \gamma_2)k_\rho^2], \quad (3)$$

$$R = \frac{\hbar^2}{2m_0} (-\sqrt{3})\gamma_{23}k_-^2, \quad (4)$$

$$S = \frac{\hbar^2}{2m_0} (2\sqrt{3})\gamma_3 k_- k_z, \quad (5)$$

where, for a magnetic field applied in the z direction we write $\mathbf{k} = -i\nabla - (e/c\hbar)\mathbf{A}$ ($e > 0$), $k_{\pm} = k_x \pm ik_y$, and $k_{\rho}^2 = k_x^2 + k_y^2$, with the vector potential in the symmetric gauge $\mathbf{A} = B/2(-y, x, 0)$. The effective masses in the z direction (m_z) and in the plane in the diagonal approximation (m_{ρ}) are defined as $m_z = 1/(\gamma_1 \mp 2\gamma_2)$ and $m_{\rho} = 1/(\gamma_1 \pm \gamma_2)$, for HH (upper sign) and LH (lower sign). The axial approximation used is $\gamma_{23} = (\gamma_2 + \gamma_3)/2$. The mixing between HH and LH states is introduced by operators R and S .

In the absence of the mixing, the HH and LH states of the disk can be classified by their envelope angular momentum m and described by the set of orthonormal envelope basis functions $\langle \mathbf{x} | m, n, \nu, m_j \rangle$:

$$\langle \mathbf{x} | m, n, \nu, m_j \rangle = \frac{\sqrt{2} J_m(k_n^m \rho)}{r |J_{m+1}(k_n^m r)|} \frac{e^{im\phi}}{\sqrt{2\pi}} \xi^{\nu}(z) u_{m_j}(\mathbf{x}). \quad (6)$$

The $J_m(k_n^m \rho)$ is the Bessel function of the first kind of order m and radial quantum number n . k_n^m represents the hole

wave vector, defined in terms of the roots (α_n^m) of the Bessel function as $k_n^m = \alpha_n^m/r$. $\xi^{\nu}(z)$ is the envelope function in the direction perpendicular to the plane of the disk. For a quantum well with infinite potential barriers and thickness w the two lowest subband wave functions for both HH and LH are $\xi(z) = \sqrt{(2/w)} \cos(\pi z/w)$ and $\xi(z) = \sqrt{(2/w)} \sin(2\pi z/w)$. The functions $u_{m_j}(\mathbf{x})$ are the periodic part of the Bloch functions and m_j designates the HH ($m_j = \pm \frac{3}{2}$) and LH ($m_j = \pm 1/2$) subbands.

When the mixing of LH and HH states is included the eigenstates of the Luttinger Hamiltonian shall be classified not by the envelope angular momenta m but by a z th component of the total angular momentum $L = m + m_j$. This is responsible for the mixing of the HH and LH states with different envelope angular momenta.

Due to inversion symmetry of the QW, the Luttinger Hamiltonian can be separated by an unitary transformation into two independent blocks, classified by the parity quantum number σ .²⁰ The simplest set of states can be written in the form of four component spinors:

$$|L, N, \sigma = \uparrow(\downarrow)\rangle = \sqrt{\frac{2}{w}} \sum_n C_{n, m_j}^{L, N, \uparrow(\downarrow)} \begin{pmatrix} f_n^{L-(3/2)}(\rho, \phi) \cos(\pi z/w) (\sin(2\pi z/w)) \left| m_j = \frac{+3}{2} \right\rangle \\ f_n^{L+(1/2)}(\rho, \phi) \cos(\pi z/w) (\sin(2\pi z/w)) \left| m_j = \frac{-1}{2} \right\rangle \\ f_n^{L-(1/2)}(\rho, \phi) \sin(2\pi z/w) (\cos(\pi z/w)) \left| m_j = \frac{+1}{2} \right\rangle \\ f_n^{L+(3/2)}(\rho, \phi) \sin(2\pi z/w) (\cos(\pi z/w)) \left| m_j = \frac{-3}{2} \right\rangle \end{pmatrix}. \quad (7)$$

The above states have a definite total angular momentum L and parity σ , with the two possible parity configurations $\sigma = \uparrow$ and $\sigma = \downarrow$. The quantum number N designates the eigenstates with the given L . States of opposite parities are orthogonal and the two parity configurations are degenerate in the absence of magnetic field. Under a suitable definition of parity operators the parity quantum number is isomorphic to the electronic spin quantum number.

We now discuss the energy spectrum of a single hole in a magnetic field. In numerical results we use parameters corresponding to the $\text{Si}_{1-x}\text{Ge}_x$ material ($x = 0.13$). The Luttinger parameters are $\gamma_1 = 5.467$, $\gamma_2 = 0.846$, and $\gamma_3 = 1.997$, obtained by linear interpolation from Si and Ge. In this example the radius of the disk is $r = 300 \text{ \AA}$ and the thickness $w = 120 \text{ \AA}$. Three different aspects determine the energy spectrum of a valence hole in a disk: the lateral confinement controlled by the radius r , the HH and LH band mixing due to the off-diagonal matrix elements of the Luttinger Hamiltonian, controlled by the effective thickness w , and the magnetic field.

The effect of the magnetic field on light and heavy holes in bulk materials and quantum dots with parabolic confinement can be solved using the algebra of the annihilation and creation operators of the harmonic oscillator.^{19,20} Instead of

working with harmonic oscillator operators suitable for parabolic confinement, we numerically diagonalize the Luttinger Hamiltonian [Eq. (1)] in the $B = 0$ basis of the disk.

Figure 1 illustrates the effect of the magnetic field and band mixing on energies of HH and LH single particle states. Figure 1(a) shows energies of hole states without band mixing and Fig. 1(b) with band mixing. In the first case the holes present an electronlike behavior and are described by the states $|m, n, \nu, m_j\rangle$. The labels in Fig. 1(a) correspond to the envelope angular momentum m and the arrows to the parity of the states. The HH states from up to the “ d ” shell and LH states from up to the “ p ” shell of the disk are shown. The states corresponding to $\pm m_j$ are degenerate. The states from different shells with $\pm m$ are degenerate only at $B = 0$ T. The finite magnetic field breaks the time reversal symmetry of the Hamiltonian and the states of $\pm m$ split as a function of B . The energies at $B = 0$ T are determined by the potential barriers in the z direction and in the plane of the disk. With the increase of the magnetic field the different energy levels evolve to form Landau Levels. Figure 1(a) shows the Landau levels LL_1 , LL_2 , and LL_3 of heavy holes (HH’s) and the first Landau level of light holes LL_1 (LH).

When band mixing is considered the description of a hole is given in terms of states $|L, N, \sigma\rangle$. The corresponding ener-

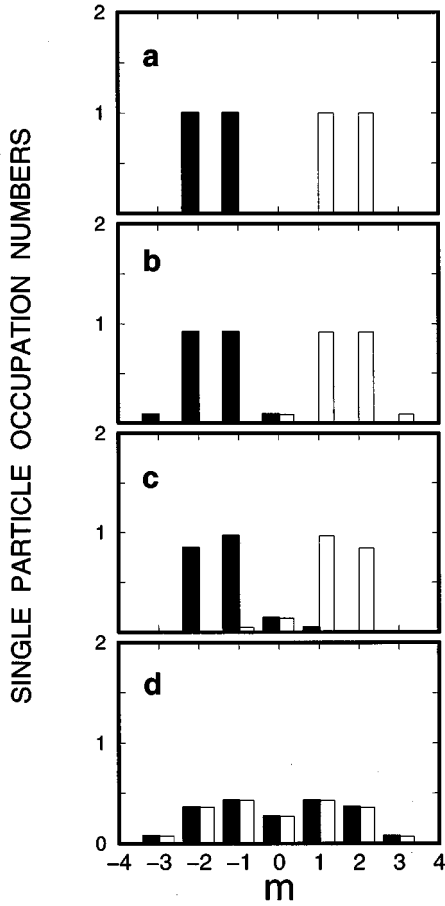


FIG. 2. Single particle occupation numbers of envelope angular momentum m for the two distinct two-hole states $|1/2, \uparrow; -1/2, \uparrow\rangle$ (white bar) and $|1/2, \downarrow; -1/2, \downarrow\rangle$ (dark bar) at $B=0$ T: (a) no subband mixing, no Coulomb interaction, (b) no subband mixing but with Coulomb interaction, (c) subband mixing included, but no Coulomb interaction (d) subband mixing and Coulomb interaction included.

in double-layer electron systems.^{15,16} Therefore the role played by the parity in interacting one-layer valence hole system is analogous with “isospin” of double-layer electron systems.

IV. SPECTRUM OF TWO HOLES IN A MAGNETIC FIELD

As an illustration of the general theory we present results of numerical calculations of the spectrum of two holes in a magnetic field. We restrict ourselves to the low energy states with a strong heavy-hole (HH_1) character as shown in Fig. 1. These single particle states are used to construct a basis of two-hole states $|L_1, N_1, \sigma_1; L_2, N_2, \sigma_2\rangle$ and the Hamiltonian is numerically diagonalized in this basis. One can alternatively classify the two-hole states by the total parity, singlet or triplet, in analogy with the isospin in double dot systems.¹⁵

An important feature of the Coulomb interaction between holes is the coupling of states with opposite parities: $\langle \downarrow\downarrow | V_{hh} | \uparrow\uparrow \rangle$. This coupling is not allowed for electrons with equivalent spin configurations. Figure 2 illustrates this effect. It presents the single particle angular momentum (m)

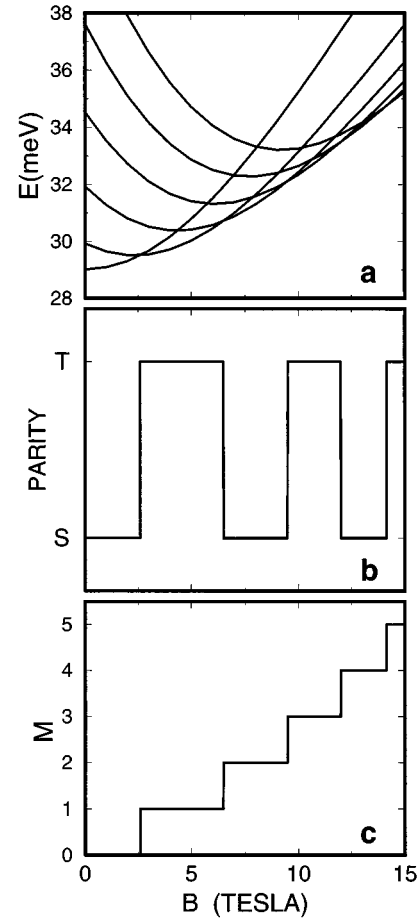


FIG. 3. (a) Energy of two-hole states without subband mixing (Coulomb interaction included) as a function of magnetic field. (b) Oscillations of the ground state between singlet and triplet parity configurations. (c) Total envelope angular momentum ($M = m_1 + m_2$) of the system as a function of magnetic field.

occupation numbers corresponding to the two-hole states: $|L_1 \uparrow, L_2 \uparrow\rangle = c_{L_1 = \frac{1}{2} \uparrow}^+ c_{L_2 = -\frac{1}{2} \uparrow}^+ |0\rangle$ and $|L_1 \downarrow, L_2 \downarrow\rangle = c_{L_1 = \frac{1}{2} \downarrow}^+ c_{L_2 = -\frac{1}{2} \downarrow}^+ |0\rangle$, for four different situations: (a) no band mixing and no Coulomb interaction, (b) no band mixing but Coulomb interaction included, (c) subband mixing included but no Coulomb interaction, and (d) both band mixing and Coulomb interactions included. In Fig. 2(a) the occupation numbers correspond to free particle states. When Coulomb interaction, but no subband mixing, is considered [Fig. 2(b)], the state $|L_1 \uparrow, L_2 \uparrow\rangle$ acquires a small projection corresponding to envelope angular momenta $m=3$ and $m=0$, not present in the free particle description. Similarly, state $|L_1 \downarrow, L_2 \downarrow\rangle$ acquires a small projection onto angular momenta $m=-3$ and $m=0$. However, no coupling exists between states $|L_1 \uparrow, L_2 \uparrow\rangle$ and $|L_1 \downarrow, L_2 \downarrow\rangle$, because without subband mixing we have $\langle L_1 \uparrow, L_2 \uparrow | V_{hh} | L_1 \downarrow, L_2 \downarrow \rangle = 0$.

Turning on the subband mixing but not the Coulomb interaction, we describe the $|L_1 \uparrow, L_2 \uparrow\rangle$ and $|L_1 \downarrow, L_2 \downarrow\rangle$ states in terms of spinors (7). Each state has now a nonzero projection on the envelope angular momenta $m = -2, -1, 0, 1, 2$, as can be seen in Fig 2(c). However, when we turn on Coulomb interaction as well as band mixing we obtain the single par-

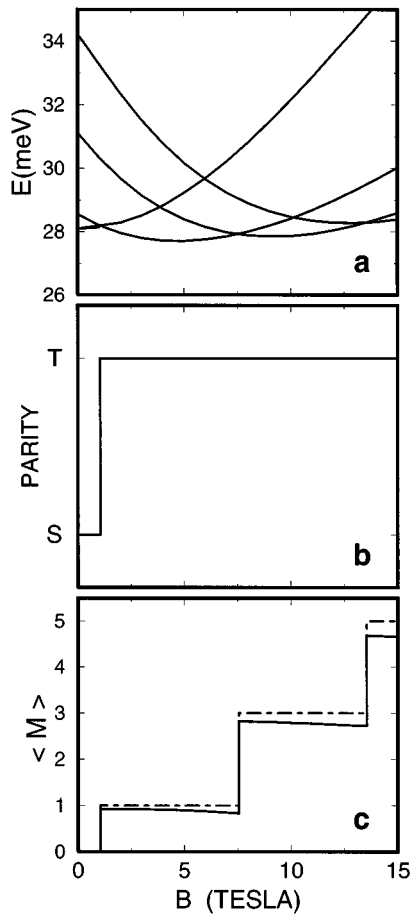


FIG. 4. (a) Energy of two-hole states with subband mixing (Coulomb interaction included) as a function of magnetic field. (b) Parity configuration of the two-hole system as a function of magnetic field. (c) Average total envelope angular momentum ($\langle M \rangle$) of the ground state (solid line).

ticle occupation numbers shown in Fig 2(d). We notice that both states are coupled, presenting very similar angular momentum distributions. This is a consequence of the fact that $\langle L_1 \uparrow, L_2 \uparrow | V_{hh} | L_1 \downarrow, L_2 \downarrow \rangle \neq 0$ when band mixing is included.

Figures 3 and 4 present the ground state energy, parity, and angular momentum of two interacting holes as a function of magnetic field. In Fig. 3(a) the interacting HH and LH holes are treated without taking into account the band mixing produced by the off-diagonal terms of the Luttinger Hamiltonian. With increasing magnetic field the parity of the ground state of the system oscillates between parity singlet and triplet configurations, as shown in Fig. 3(b). This is known to be a consequence of the Coulomb interaction between the particles.^{7,21–24} Figure 3(c) shows that the total envelope angular momentum ($M = m_1 + m_2$) of the system changes with the parity configuration, with even values of M associated with singlet states and odd values of M with triplet states.

When band mixing is included we obtain a different behavior, shown in Fig. 4. The main result of the band mixing is the removal of the oscillatory behavior of the parity of the ground state. Once the singlet parity ground state changes to a triplet at $B \approx 1$ T the change of parity from triplet back to singlet does not occur. The angular momentum L of the

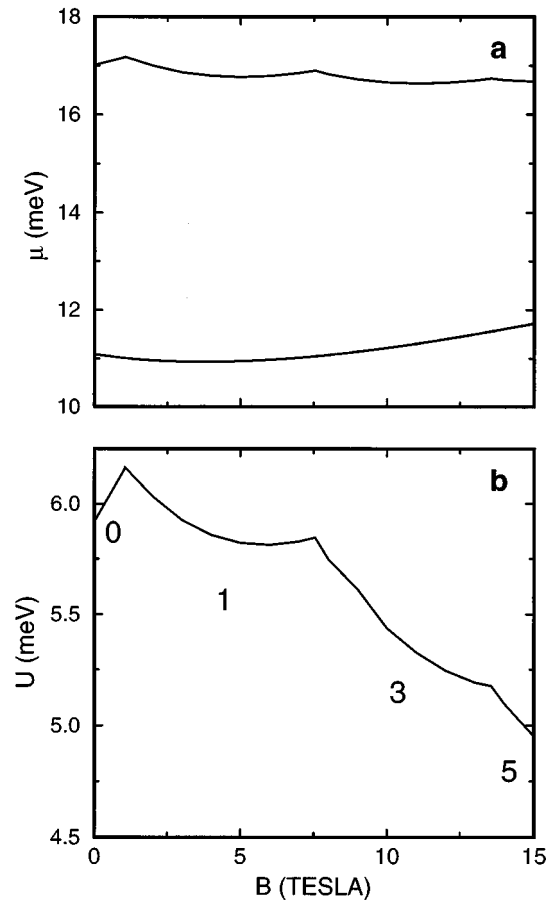


FIG. 5. (a) The magnetic field dependence of the chemical potential $\mu(N)$, for $N=2$ (upper curve) and $N=1$ (lower curve). (b) Charging energy U of the two-hole system as a function of the magnetic field.

ground state still changes as a function of the magnetic field, as shown in Fig. 4(a), with all ground states for $B > 1$ T having a parity configuration $|\downarrow\downarrow\rangle$ [Fig. 4(b)]. The band mixing and the Coulomb interaction break the degeneracy of the three triplet configurations. The fact that the magnetic field forces the parity configuration $|\downarrow\downarrow\rangle$ to be the ground state can be understood in terms of the single-hole results of Fig. 1. In that case the magnetic field increased the band mixing of hole states with parity \downarrow more than those of parity \uparrow , causing their effective masses to increase. Therefore the two-hole states made of $\sigma = \downarrow$ have a lower energy than those of $\sigma = \uparrow$. In Fig. 4(c) we present the average envelope angular momentum $\langle M \rangle$ of the hole states (solid line). The dashed line is plotted as a reference and it corresponds to a situation where no band mixing is present. We observe that odd values of M correspond to the $|\downarrow\downarrow\rangle$ states. The increasing separation of these two lines, as B is increased, is another indication that the magnetic field increases the band mixing of these states. The band mixing of holes can be considered as an effective “Zeeman effect” that causes the ground states of the system to remain a triplet state, associated with only odd values of angular momenta.

The effects of hole-hole interactions can be measured via single electron capacitance spectroscopy (SECS). SECS measures the chemical potential of the dot

$\mu(N) = E_{\text{GS}}(N) - E_{\text{GS}}(N-1)$ as a function of the number of holes N in the dot. In Fig. 5(a) we show the dependence of $\mu(N)$ on the magnetic field for $N=1,2$. Figure 5(b) shows the magnetic field dependence of the charging energy $U = E_{\text{GS}}^{\text{int}}(N=2) - E_{\text{GS}}^{\text{nonint}}(N=2)$ for two holes. The dominant total envelope angular momenta (M) of the corresponding ground states are indicated. As the total angular momentum of the system increases as a function of magnetic field the holes tend to move farther apart from each other, therefore decreasing their interaction energy. The charging energy would be responsible for the operation of a single-hole transistor.

V. CONCLUSIONS

We investigated the electronic states, energies, and capacitance spectra of interacting valence holes in quantum disks in a magnetic field. We have shown that hole states can be classified by parity instead of spin. The magnetic field plays an important role in controlling the mixing between different parity states. The Coulomb scattering of holes contains parity conserving and parity flipping contributions. Therefore the Hamiltonian is a combination of charge-charge and parity-parity interaction terms, in analogy with the iso-

spin in double-layer electronic systems. The exact diagonalization studies of this Hamiltonian were carried out for up to two holes in SiGe quantum disk. The ground state energy shows cusps associated with magnetic field induced changes of the ground state angular momentum. We find that the parity triplet-singlet transition, characteristic of electrons in such structures, is not present in the case of holes. The magnetic field dependence of the charging energy in a capacitance spectra is analyzed.

ACKNOWLEDGMENTS

One of the authors (L.G.C.R.) acknowledges CNPq (Brazil) for financial support and J.A.B. acknowledges RHAECNPq (Brazil) and Institute for Microstructural Sciences-NRC (Canada) for partial financial support.

APPENDIX

The external magnetic field induces scattering among the single-hole basis states that conserve the angular momentum (L) and parity (σ). The magnetic field dependent parts of the matrix elements corresponding to the operators P_{\pm} , R , and S are, respectively,

$$\langle \sigma' N' L' | U^{P_{\pm}} | LN \sigma \rangle = \frac{\hbar^2}{2m_0} (\gamma_1 \pm \gamma_2) \sum_{m_j} \sum_{n, n'} C_{n' m_j}^{*LN' \sigma} C_{nm_j}^{LN \sigma} \left\{ \frac{\Omega^2}{4} \langle n' m | \rho^2 | mn \rangle - \Omega m \delta_N^{n'} \right\} \delta_L^{L'} \delta_{\sigma'}^{\sigma}, \quad (\text{A1})$$

$$\begin{aligned} \langle \sigma' N' L' | U^R | LN \sigma \rangle &= \frac{\hbar^2}{2m_0} (-\sqrt{3}) \gamma_{23} \delta_L^{L'} \delta_{\sigma'}^{\sigma} \sum_{n, n'} \left\{ \sum_{m_j = -3/2, -1/2} C_{n' (m_j+2)}^{*LN' \sigma} C_{nm_j}^{LN \sigma} \left\langle n' (m-2) \left| \left(\Omega m - \frac{\Omega^2 \rho^2}{4} + \Omega \rho \frac{\partial}{\partial \rho} \right) \right| mn \right\rangle \right. \\ &+ \left. \sum_{m_j = 3/2, 1/2} C_{n' (m_j-2)}^{*LN' \sigma} C_{nm_j}^{LN \sigma} \left\langle n' (m+2) \left| \left(-\Omega m - \frac{\Omega^2 \rho^2}{4} + \Omega \rho \frac{\partial}{\partial \rho} \right) \right| mn \right\rangle \right\}, \quad (\text{A2}) \end{aligned}$$

$$\begin{aligned} \langle \sigma' N' L' | U^S | LN \sigma \rangle &= \frac{\hbar^2}{2m_0} (2\sqrt{3}) \gamma_3 \left(\frac{-4\Omega}{3W} \right) \sigma \delta_L^{L'} \delta_{\sigma'}^{\sigma} \sum_{n, n'} \left\{ \sum_{m_j = -3/2, 1/2} C_{n' (m_j+1)}^{*LN' \sigma} C_{nm_j}^{LN \sigma} \text{sgn}(m_j) \langle n' (m-1) | \rho | mn \rangle \right. \\ &- \left. \sum_{m_j = -1/2, 3/2} C_{n' (m_j-1)}^{*LN' \sigma} C_{nm_j}^{LN \sigma} \text{sgn}(m_j) \langle n' (m+1) | \rho | mn \rangle \right\}, \quad (\text{A3}) \end{aligned}$$

where $L = m + m_j$, $\sigma(\uparrow) \equiv 1$, $\sigma(\downarrow) \equiv -1$, $\Omega = e_B^{-2}$, and $e_B = \hbar c / eB$)^{1/2}. The function $\text{sgn}(m_j)$ stands for the sign of m_j . The matrix elements involving vectors $|mn\rangle$ are calculated in terms of scalar products between Bessel functions $J_m(k_n^m \rho)$ [Eq. (6)].

In order to obtain the Coulomb matrix elements we use the expansion of Coulomb interaction in terms of Bessel functions

$$\frac{1}{|\mathbf{x} - \mathbf{x}'|} = \sum_{l=-\infty}^{\infty} \int_0^{\infty} dq e^{il(\phi - \phi')} J^l(q\rho) J^l(q\rho') e^{-q|z - z'|}, \quad (\text{A4})$$

the Coulomb matrix elements among hole states $|j_i\rangle = |L_i, N_i, \sigma_i\rangle$ are written as

$$\langle j_1 j_2 | V_{hh} | j_3 j_4 \rangle = \frac{e^2}{\epsilon_0 r} \sum_{m_j^1} \sum_{m_j^2} \sum_{n^1, n^2, n^3, n^4} C_{n^1 m_j^1}^{*L_1 N_1 \sigma_1} C_{n^4 m_j^4}^{L_4 N_4 \sigma_4} C_{n^2 m_j^2}^{*L_2 N_2 \sigma_2} C_{n^3 m_j^3}^{L_3 N_3 \sigma_3} \int_0^{\infty} dQ G_{n^1 n^4}^{L_1 L_4 m_j^1}(Q) G_{n^3 n^2}^{L_3 L_2 m_j^2}(Q) \chi_{\sigma_1 \sigma_2 \sigma_3 \sigma_4}^{m_j^1 m_j^2} \left(\frac{Q}{r} \right), \quad (\text{A5})$$

where ϵ_0 is the static dielectric constant of $\text{Si}_{0.87}\text{Ge}_{0.13}$ and r is the radius of the disk. We define $Q = rq$ and

$$G_{nn'}^{LL'm_j}(Q) = \frac{2 \int_0^1 ds s J_{L-m_j}(k_n^{L-m_j} r s) J_{L-L'}(q r s) J_{L'-m_j}(k_{n'}^{L'-m_j} r s)}{|J_{L-m_j+1}(k_n^{L-m_j} r) J_{L'-m_j+1}(k_{n'}^{L'-m_j} r)|}, \quad (\text{A6})$$

with $\rho = sr$. The form factor $\chi_{\sigma_1 \sigma_2 \sigma_3 \sigma_4}^{m_j^1 m_j^2}[Q(w/r)]$ can be written as

$$\chi_{\sigma_1 \sigma_2 \sigma_3 \sigma_4}^{m_j^1 m_j^2}(q) = \int_{-w/2}^{w/2} dz' \xi_{\sigma_2}^{m_j^2}(z') \xi_{\sigma_3}^{m_j^2}(z') \int_{-w/2}^{w/2} dz \xi_{\sigma_1}^{m_j^1}(z) \xi_{\sigma_4}^{m_j^1}(z) e^{-q|z-z'|}. \quad (\text{A7})$$

*Permanent address: Instituto de Física ‘‘Gleb Wataghin,’’ UNICAMP, Campinas, Brazil, 13081-970.

†Permanent address: Institute of Physics, Technical University of Wrocław, Wybrzeże Wyspiańskiego 27, 50-370, Wrocław, Poland.

¹A. A. Darnhuber, J. Stangl, G. Bauer, D.J. Lockwood, J.P. Noel, P.D. Wang, and C.M. Sotomayor Torres (unpublished).

²G. Abstreiter, P. Schittenhelm, C. Engel, E. Silveira, A. Zrenner, D. Meertens, and W. Jager, Proceedings of the 9th International Winterschool on New Developments in Solid State Physics, Mauterndorf, 1996 [Semicond. Sci. Technol. **11**, 1521 (1996)].

³A. Zaslavsky, K.R. Milkove, Y.H. Lee, B. Ferland, and T.O. Sedgwick, Appl. Phys. Lett. **67**, 3921 (1995); A. Zaslavsky, T.P. Smith III, D.A. Grutzmacher, S.Y. Lin, T.O. Sedgwick, and D.A. Syphers, Phys. Rev. B **48**, 15 112 (1993).

⁴H.C. Liu, P. Landheer, M. Buchanan, and D.C. Houghton, Appl. Phys. Lett. **52**, 1809 (1989).

⁵M. Arafa, P. Fay, K. Ismail, J.O. Chu, B.S. Meyerson, and I. Adesida, IEEE Electron Device Lett. **17**, 124 (1996).

⁶D.C. Houghton, G.C. Aers, S.R. Eric Yang, E. Wang, and N.L. Rowell, Phys. Rev. Lett. **75**, 866 (1995).

⁷R.C. Ashoori, H.L. Stormer, J.S. Weiner, L.N. Pfeiffer, K.W. Baldwin, and K.W. West, Phys. Rev. Lett. **71**, 613 (1993); Bo Su, V.J. Goldman, and J.E. Cunningham, Science **255**, 313 (1992).

⁸W. Hansen, T.P. Smith III, K.Y. Lee, J.A. Brum, C.M. Knoedler, J.M. Hong, and D.P. Kern, Phys. Rev. Lett. **62**, 2168 (1989).

⁹H. Drexler, D. Leonard, W. Hansen, J.P. Kotthaus, and P.M. Petroff, Phys. Rev. Lett. **73**, 2252 (1994).

¹⁰K.J. Vahala and P.C. Sercel, Phys. Rev. Lett. **65**, 239 (1990); P.C. Sercel and K.J. Vahala, Phys. Rev. B **42**, 3690 (1990).

¹¹D.A. Broido, A. Cros, and U. Rössler, Phys. Rev. B **45**, 11 395 (1992).

¹²T. Darnhofer, U. Rössler, and D.A. Broido, Phys. Rev. B **52**, 14 376 (1995); T. Darnhofer *et al.*, *ibid.* **53**, 13 631 (1996).

¹³F.B. Pedersen and Yia-Chung Chang, Phys. Rev. B **53**, 1507 (1996).

¹⁴For recent reviews and references see M. Kastner, Phys. Today **46**, 24 (1993); T. Chakraborty, Comments Condens. Matter Phys. **16**, 35 (1992).

¹⁵J.J. Palacios and P. Hawrylak, Phys. Rev. B **51**, 1769 (1995).

¹⁶A. H. MacDonald, P. M. Platzman, and G. S. Boebinger, Phys. Rev. Lett. **65**, 775 (1990).

¹⁷J.-Y. Marzin, J.-M. Gerard, P. Voisin, and J.A. Brum, in *Strained-Layer Superlattices: Physics*, edited by T.P. Pearsall, Semiconductor and Semimetals Vol. 32 (Academic Press, New York, 1990), p. 56.

¹⁸J.M. Luttinger and W. Kohn, Phys. Rev. **97**, 869 (1955).

¹⁹J.M. Luttinger, Phys. Rev. **102**, 1030 (1956).

²⁰D. Broido and L.J. Sham, Phys. Rev. B **31**, 888 (1985).

²¹M. Wagner, U. Merkt, and A.V. Chaplik, Phys. Rev. B **45**, 1951 (1992); P.A. Maksym and Tapash Chakraborty, *ibid.* **45**, 1947 (1992).

²²Garnett W. Bryant, Phys. Rev. Lett. **59**, 1140 (1987).

²³D. Pfannkuche and R. Gerhardt, Phys. Rev. B **44**, 13 132 (1991).

²⁴P. Hawrylak, Phys. Rev. Lett. **71**, 3347 (1993).